
**Submission code: 0RZ9XD74B4**

See this and other abstracts on our website: https://home.sbgf.org.br/Pages/resumos.php

# REM-Based Frequency-Domain Seismic Modeling and Imaging

**DANIEL REVELO APRAEZ (SENAI CIMATEC), Reynam C. Pestana (UFBA)**

## REM-Based Frequency-Domain Seismic Modeling and Imaging




# Abstract

Seismic frequency responses can be computed by solving the wave equation in the frequency domain or by Fourier transforming time-domain wavefields. While the frequency-domain approach requires solving large sparse systems — computationally expensive at high frequencies — explicit time integration offers an alternative, though traditional Taylor-based expansions suffer from instability at large time steps. To overcome this, we adopt the Rapid Expansion Method (REM) with Chebyshev polynomials for a more stable and accurate solution for second-order time integration. We propose a novel strategy that directly retrieves frequency components from Chebyshev coefficients using an analytical Fourier representation based on Bessel functions. This enables precomputation of all desired frequencies, reducing computational cost. Numerical tests show excellent agreement with conventional time-domain results and demonstrate the method's applicability in seismic migration.


# Introduction

Computational solvers for the Helmholtz equation are crucial in seismology, acoustics and other wave-based fields, particularly for single-frequency modeling in seismic inversion. Frequency-domain Full-Waveform Inversion (FWI) (Tarantola, 1984) is often favored for its computational efficiency, requiring fewer frequencies for inversion. However, solving large sparse systems in complex media remains a significant challenge. Direct solvers, while allowing factor reuse, demand substantial memory. Iterative methods offer better scalability but are prone to convergence issues, especially at high frequencies (Plessix, 2007). Alternatively, frequency responses can be obtained via Discrete Fourier Transform (DFT) of time-domain wavefields using explicit schemes. Standard low-order Finite-Difference (FD) time integration often causes dispersion errors with high-order spatial schemes, requiring small time steps and increasing computational costs. The Rapid Expansion Method (REM) (Kosloff et al., 1989) improves time extrapolation by expanding the wavefield in Chebyshev polynomials, effectively eliminating dispersion with sufficient terms. Comparisons confirm its superiority over second-order truncated Taylor series expansions (Pestana and Stoffa, 2010).

Another frequency response modeling technique uses the running summation algorithm (Chu and Stoffa, 2012), applying REM to temporal derivatives and the pseudospectral method for spatial derivatives. Since REM optimally solves second-order wave equations using Chebyshev polynomials (Pestana and Stoffa, 2010), applying a DFT to the REM-computed time-domain wavefield yields a frequency-domain formulation with modified summation coefficients. These coefficients are the DFT of the time-domain expansion terms, enabling direct frequency response computation from the Chebyshev polynomial expansion, bypassing discrete time snapshots (Chu and Stoffa, 2012). In this work, we introduce a novel REM-based frequency response modeling approach. Unlike the approach proposed by Chu and Stoffa (2012), which derives summation coefficients from the Fourier transform of a convolution involving the Bessel function and the source wavelet, we analytically obtain them from the transform of the Bessel function alone. We describe a forward-modeling solver for the acoustic wave equation using a modified Chebyshev expansion with Bessel-function time dependence, leading to an efficient REM-based frequency response formulation. Numerical experiments validate the proposed method, demonstrating its effectiveness in seismic imaging.

## Theory

The REM, based on Chebyshev expansions, provides efficient time integration for second-order wave equations, such as the constant-density acoustic wave equation

$$\frac{\partial^2 P(\mathbf{x},t)}{\partial t^2} = -L^2 P(\mathbf{x},t) + f(\mathbf{x},t), \quad \text{with} \quad L^2 = -c^2\left(\frac{\partial^2}{\partial x^2} + \frac{\partial^2}{\partial y^2} + \frac{\partial^2}{\partial z^2}\right), \tag{1}$$

where $\mathbf{x} = (x, y, z)$, $t$ is time, $c = c(\mathbf{x})$ is the velocity, $P(\mathbf{x},t)$ is the pressure wavefield, and $f(\mathbf{x},t)$ denotes the source term. Applying the Fourier transform to Eq. 1 yields $P(\mathbf{x},\omega) = G(\mathbf{x},\omega)f(\mathbf{x},\omega)$, where $G(\mathbf{x},\omega) = 1/\left(L^2 - \omega^2\right)$ is the frequency-domain Green's function. The corresponding time-domain expression, obtained via the residue theorem, is $G(\mathbf{x},t) = \sin(Lt)/L$. If the source term is separable as $f(\mathbf{x},t) = g(\mathbf{x})s(t)$, then the solution to Eq. 1 becomes (Kosloff et al., 1989)

$$P(\mathbf{x},t) = H(\mathbf{x},t) * s(t), \quad \text{with} \quad H(\mathbf{x},t) = \frac{\sin(Lt)}{L} g(\mathbf{x}). \tag{2}$$

Using a modified Chebyshev expansion of the sine function, $H(\mathbf{x},t)$ is approximated as

$$H(\mathbf{x},t) = \frac{1}{R}\sum_{k=0}^{\infty} J_{2k+1}(tR)\,\frac{R}{iL}\,Q_{2k+1}\left(\frac{iL}{R}\right) g(\mathbf{x}), \tag{3}$$

where $J_{2k+1}$ are odd-order Bessel functions, and $Q_{2k+1}$ are modified Chebyshev polynomials defined by the recurrence $Q_{2k+1}(\xi) = 2\left[1 + 2\xi^2\right] Q_{2k-1}(\xi) - Q_{2k-3}(\xi)$, with $Q_1(\xi) = \xi$, $Q_3(\xi) = 3\xi + 4\xi^3$, and $\xi = iL/R$. The scalar $R$, exceeding the eigenvalue range of $L$, approximated in 2D by $R \approx \pi c_{\text{max}}\sqrt{(1/\Delta x)^2 + (1/\Delta z)^2}$, and the condition $M > tR$, using only odd terms for convergence (Tal-Ezer et al., 1987), are crucial for the method.

From Eq. 2, the frequency-domain pressure wavefield is $P(\mathbf{x},\omega) = H(\mathbf{x},\omega)s(\omega)$. To compute this, we apply a Fourier transform to Eq. 3. which only affects the Bessel functions, resulting in

$$H(\mathbf{x},\omega) = \frac{1}{R}\sum_{k=0}^{\infty} B_{2k+1}(\omega)\,\frac{R}{iL}\,Q_{2k+1}\left(\frac{iL}{R}\right) g(\mathbf{x}), \tag{4}$$

where $B_{2k+1}(\omega)$ is the temporal Fourier transform of $J_{2k+1}(tR)$, given by

$$B_{2k+1}(\omega) = \frac{1}{R}\,\frac{e^{-i\left[(2k+1)\sin^{-1}(\omega/R)\right]}}{\sqrt{1-(\omega/R)^2}} \quad \text{if } |\omega/R| < 1, \text{and zero otherwise.} \tag{5}$$

With Eq. 4, we obtain the expression for the frequency-domain response, given by

$$P(\mathbf{x},\omega) = \frac{1}{R}\sum_{k=0}^{M} s(\omega)\,B_{2k+1}(\omega)\,\Omega_{2k+1}(\mathbf{x}), \quad \text{with} \quad \Omega_{2k+1}(\mathbf{x}) = \frac{R}{iL} Q_{2k+1}\left(\frac{iL}{R}\right) g(\mathbf{x}). \tag{6}$$

Based on the Chebyshev recurrence and initial values, the polynomial terms are computed via the recurrence $\Omega_{2k+1}(\mathbf{x}) = 2\left[1 + 2\left(-L^2/R^2\right)\right]\Omega_{2k-1}(\mathbf{x}) - \Omega_{2k-3}(\mathbf{x})$, initiated by $\Omega_1(\mathbf{x}) = g(\mathbf{x})$ and $\Omega_3(\mathbf{x}) = \left[3 + 4\left(-L^2/R^2\right)\right] g(\mathbf{x})$. Although $\Omega_{2k+1}$ contains $1/iL$, the recurrence only envolves $-L^2$ (evaluated once per term), which dominates the cost in Eq. 6. Our f-REM computes $B_{2k+1}(\omega)$ analytically (Eq. 5) for each frequency and odd index, multiplying it by the precomputed, frequency-independent $\Omega_{2k+1}(\mathbf{x})$. The wavefield $P(\mathbf{x},\omega)$ is the sum of $M/2$ odd terms in Eq. 6. This method, unlike conventional frequency-domain modeling, decouples spatial discretization, allows multi-source encoding across frequencies, and extends to complex media without restrictive assumptions.

As an application of f-REM-derived frequency responses, we employ the linear modeling based on the Born approximation (Yao and Jakubowicz, 2016). The scattered wavefield is $\mathbf{d} = \mathbf{Lm}$, where

$\mathbf{L}$ is the discretized modeling operator and $\mathbf{m}$ the reflectivity model. Each matrix element is given by $l_{ij} = \frac{\omega^2}{c_0^2(\mathbf{x}_j)} s(\omega) G_0(\mathbf{x}_j, \omega; \mathbf{x}_s) G_0(\mathbf{x}_j, \omega; \mathbf{x}_{ri})$, with $\mathbf{x}_j$ denoting the $j$-th grid point, $\mathbf{x}_s$ the source location, and $\mathbf{x}_{ri}$ the $i$-th receiver. Migration uses the adjoint operator, and a balanced image is obtained via diagonal Hessian preconditioning: $\mathbf{m}_{\text{mig}} = (\mathbf{H}_0 + \lambda \mathbf{I})^{-1} \mathbf{L}^{\mathsf{T}} \mathbf{d}_{\text{obs}}$, where $\mathbf{H}_0 = \text{diag}\{\mathbf{L}^{\mathsf{T}}\mathbf{L}\}$.

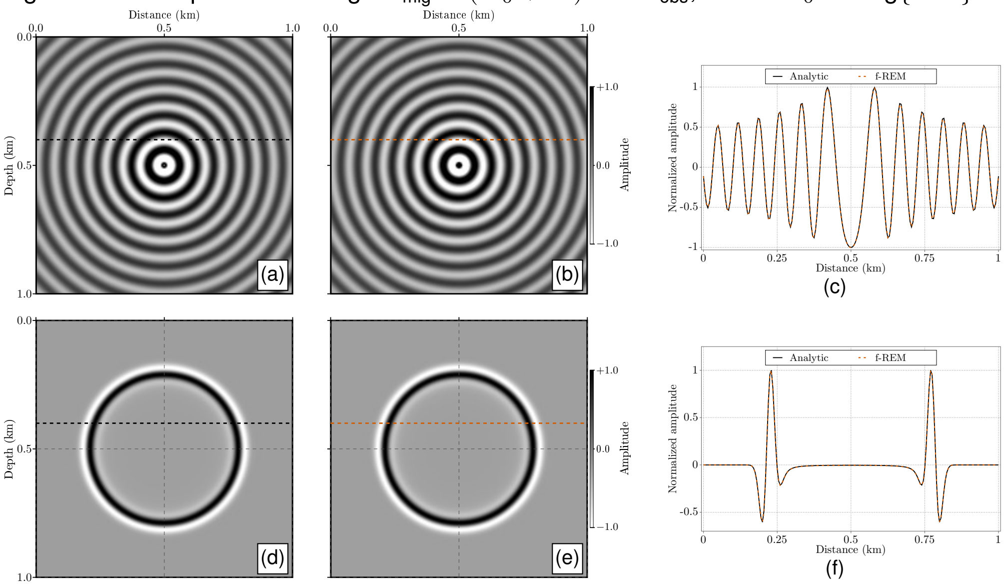


Figure 1: Real part of frequency response: (a) analytic solution, (b) f-REM. Time-domain snapshots: (d) analytic solution, (e) f-REM. Normalized amplitude trace comparison ($z = 400$ m): (c) frequency-domain responses, (f) time-domain snapshots.

## Results

We evaluated our f-REM method by computing frequency responses for two velocity models of increasing complexity. To validate the frequency-domain results, we applied an inverse Fourier transform and compared them with time-domain REM wavefields. A 12th-order finite-difference scheme was used for the Laplacian operator, and absorbing boundary conditions were applied.

Initially, we tested f-REM on a homogeneous 2D isotropic model ($201 \times 201$ grid points, velocity $2000$ m/s). Using a $30$ Hz Ricker wavelet with a source at $\mathbf{x}_s = (500, 500)$m, the f-REM frequency responses showed excellent agreement with the analytic solution (Figures 1(a)-(b)). The normalized cross-correlation (NCC) value was $0.998$. A trace comparison is provided in Figure 1(c). After inverse Fourier transform, the time-domain wavefields at $t = 0.18$ s (Figures 1(d)-(e)) also exhibited high similarity (NCC = $0.997$), further confirmed by seismic trace comparison (Figure 1(f)). Next, we applied f-REM to the complex Marmousi model ($369 \times 375$ samples and spatial sampling of $25$ m in $x$ and $8$ m in $z$). A $9$ Hz Ricker wavelet was injected at $\mathbf{x}_s = (4600, 0)$m, and the resulting time-domain wavefields were compared with REM. The real and imaginary parts of the $9.5$ Hz frequency responses are shown in Figures 2(c)-(d), while time-domain snapshots (Figures 2(e)-(f)) displayed strong agreement (NCC = $0.999$), as seen in Figure 2(h). Furthermore, we applied f-REM for adjoint migration, using 190 frequencies from $0.167$ Hz to $31.5$ Hz. The resulting high-quality migrated image (Figure 2(g)) demonstrates f-REM's capability in complex seismic modeling.

The numerical results validate the proposed f-REM method for efficient frequency-domain seismic modeling. By eliminating time-marching and requiring minimal memory ($O(nx, nz)$), it demonstrates scalability for large, high-frequency problems and straightforward 3D extension. While a Laplacian operator was used spatially, a pseudospectral approach could further enhance performance, particularly in 2D. The high-quality migrated image derived from the frequency responses further confirms the method's effectiveness.

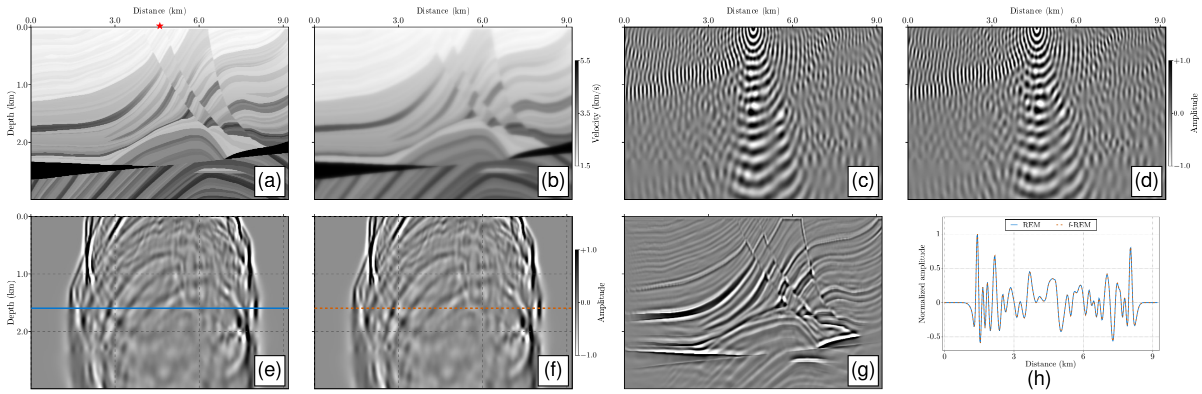


Figure 2: (a) Marmousi P-wave velocity model and (b) background model. f-REM $9.5\,\mathrm{Hz}$ frequency responses: (c) real part, (d) imaginary part. Time-domain snapshots: (e) REM, (f) f-REM. (g) Migrated image. (h) Normalized amplitude trace comparison ($z = 1600\,\mathrm{m}$).

## Conclusions

We proposed a new REM-based method for frequency response modeling in the frequency-space domain. By analytically transforming the Bessel function, we derive frequency-domain Chebyshev coefficients, allowing efficient multi-frequency computation. Validated for accuracy and efficiency on synthetic data, its successful application in seismic imaging underscores its potential as a flexible tool for seismic modeling and waveform inversion, with natural extensions to 3D and anisotropic media.

## Acknowledgments

This research was conducted within the framework of the Marchenko project, with financial support from CENPES/Petrobras. We would like to thank CENPES and SENAI CIMATEC for granting permission to publish this research. Reynam C. Pestana acknowledges financial support from CNPq through the INCT-GP.

## References

Chu, C., and P. Stoffa, 2012, Efficient 3D frequency response modeling with spectral accuracy by the rapid expansion method: Geophysics, **77**, T117–T123.

Kosloff, D., A. Q. Filho, E. Tessmer, and A. Behle, 1989, Numerical solution of thr acoustic and elastic wave equation by a new rapid expansion method: Geophysical Prospecting, **37**, 383–384.

Pestana, R. C., and P. L. Stoffa, 2010, Time evolution of the wave equation using rapid expansion method: Geophysics, **75**, T121–T131.

Plessix, R. E., 2007, A Helmholtz iterative solver for 3D seismic imaging problems: Geophysics, **72**, SM185–SM194.

Tal-Ezer, H., D. Kosloff, and Z. Koren, 1987, An accurate scheme for seismic forward modelling: Geophysical Prospecting, **35**, 479–490.

Tarantola, A., 1984, Inversion of seismic reflection data in the acoustic approximation: Geophysics, **49**, 1259–1266.

Yao, G., and H. Jakubowicz, 2016, Least-squares reverse-time migration in a matrix-based formulation: Geophysical Prospecting, **64**, 611–621.